TOPICAL REVIEW — Magnetism, magnetic materials, and interdisciplinary research

Magnetic microbubble: A biomedical platform co-constructed from magnetics and acoustics*

Yang Fang(杨 芳)[a], Gu Zhu-Xiao(顾竹笑)[b], Jin Xin(金 熙)[a], Wang Hao-Yao(王皓瑶)[a], and Gu Ning(顾 宁)[a]†

[a] *Jiangsu Key Laboratory for Biomaterials and Devices, State key Laboratory of Bioelectronics, School of Biological Science and Medical Engineering, Southeast University, Nanjing* 210096, *China*

[b] *Key Laboratory of Developmental Genes and Human Diseases, Ministry of Education, Medical School, Southeast University, Nanjing* 210009, *China*

(Received 5 August 2013)

Generation of magnetic micrbubbles and their basic magnetic and acoustic mechanism are reviewed. The ultrasound (US) and magnetic resonance (MR) dual imaging, the controlled therapeutic delivery, as well as theranostic multifunctions are all introduced based on recent research results. Some on-going research is also discussed.

Keywords: magnetic nanoparticles, microbubbles, magnetic micobubbles, magnetics, acoustics, biomedical application

PACS: 43.25.+y, 43.35.RW, 85.70.Ec, 87.50.–a **DOI:** 10.1088/1674-1056/22/10/104301

1. Introduction

Magnetic microbubbles exhibit many interesting acoustic and magnetic properties based on one microbubble conconstructed platform. The excellent ultrasonic and magnetic responses are beneficial for the biomedical applications. With the development of micro- and nano-delivery carriers, much research has demonstrated that both microbubbles (MBs) and magnetic nanoparticles (MNPs) can individually be regarded as effective imaging contrast agents and drug delivery carriers.[1–3] MBs are the gas-filled microspheres with diameter of several micrometers due to the requirement of *in vivo* application. When an ultrasonic energy field is applied, MBs can oscillate and vibrate; thus may reflect ultrasound waves to be distinguished from surrounding tissues. This strong ultrasonic scattering of MBs make them become as the most effective type of ultrasound imaging contrast agent to enhance the ultrasound imaging.[4] Besides, with the modified shell, the drugs, DNA or antibodies can be loaded into the MBs, which opened up the possibility for molecular imaging, targeted drug delivery, gene therapy, thrombolysis, and focused ultrasound surgery.[5] Besides the excellent acoustic characteristic, gas-filled MBs have also been demonstrated to be useful in magnetic resonance (MR) imaging when the susceptibility of the gas differs from that of the surrounding medium. The localized perturbations created by MBs can act as susceptibility contrast agent to shorten T_2 and T_2^*. Especially, some theoretical and experimental studies have shown that the magnetic susceptibility sensitivity of MBs can be improved by embedding magnetically active particles around the microbubbles' shell.[6]

Magnetic particles of micro- or nano-scale have been widely investigated for biomedical applications. When the size of magnetic particles is below 100 nm, the magnetic ordering at the surface will be changed. For ferromagnetic nanoparticles, a surface spin glass-like state due to magnetic frustration has been found. Among the ferromagnetic nanoparticles, the superparamagnetic iron oxide (SPIO) magnetic particles exhibit no remanence or coercivity. Superparamagnetism is necessary in drug delivery because once the external magnetic field is removed, magnetization disappears and thus agglomeration is avoided.[7,8] Because of special superparamagnetic features of MNPs, they can be used to function at the cellular and molecular level of biological interactions. We can call these MNPs as biomedical magnetic nanoparticles (BMNPs). These BMNPs offer some attractive possibilities in clinical MR imaging contrast agents enhancement, molecular imaging, magnetically targeted release of therapeutic agents, hyperthermia, as well as magnetic field assisted radionuclide therapy, etc.[9]

Recent advances in biomedical applications have driven the development of multifunctional nano-, or micro-multiscale delivery carriers. The integration of nano- and micro-multiscale technology has resulted in new devices in biomedical applications.[10–12] Combination of dual-phase character of MNPs and MBs, magnetic microbubble (MMBs) formulations have been developed as novel approach for delivery systems, analytical biochemistry and *in vitro*/*vivo* theranostics. In this review, we mainly discuss the fabrication and biomedi-

*Project supported by the National Basic Research Program of China (Grant Nos. 2011CB933503 and 2013CB733804), the National Natural Science Foundation of China (Grant No. 31000453), and the Fundamental Research Funds for Central Universities (Grant No. 2013CB733804).

†Corresponding author. E-mail: guning@seu.edu.cn

© 2013 Chinese Physical Society and IOP Publishing Ltd

cal applications of MMBs. First, we will give an overview of the basic properties of MBs, MNPs, and MMBs individually, which may be most critical to biomedical applications. Second, we will explain the acoustic and magnetic interaction of the combined agents resulting from magnetic microbubble coconstructure. Finally, how these properties can be exploited to create and improve biomedical diagnostic techniques and treatments will be discussed.

2. Magnetic nanoparticles and magnetic characteristics

2.1. Preparation, surface modification, assembly of magnetic nanoparticles

When the size of the MNPs is below a critical value (typically around 10 nm–20 nm), each MNP has a large constant magnetic moment and behaves like a giant paramagnetic atom with a fast response to applied magnetic fields with negligible residual magnetism and coercivity. These features make superparamagnetic nanoparticles very attractive for a broad range of biomedical applications because the risk of agglomeration is negligible at room temperature.[13] In order to obtain reliable BMNPs, the enhanced magnetic moments and superparamagnetism must be considered, which must have optimum composition, appropriate surface charge, shape, size, and colloidal stability in a biological environment, biocompatibility, and specific targeting capability.[14,15]

Recently, techniques and procedures for producing BMNPs including Fe_3O_4, γ-Fe_2O_3 have advanced considerably. In order to obtain shape-controlled, highly stable, and monodisperse BMNPs, there are many synthetic routes to be developed. These synthetic methods can be classified into two categories. One is the MNPs produced from solution or vapor phases. The other is the MNPs produced by composites consisting of MNPs dispersed in the nano- or micro-sized organic or inorganic spherical matrixes.

Methods for MNPs produced from solution mainly include co-precipitation, thermal decomposition, microemulsion, hydrothermal synthesis techniques. Precipitation from solution methods allow the preparation of MNPs with rigorous control of size and shape in a simple way, and thus are very appropriate for use in biomedical applications. Uniform particles are usually prepared via homogeneous precipitation reactions, a process that involves the separation of the nucleation and growth of the nuclei.[16] In a homogeneous precipitation, a short single burst of nucleation occurs when the concentration of constituent species reaches critical supersaturation. Then, the nuclei obtained are allowed to grow uniformly by diffusion of solutes from the solution to their surface until the final size is attained. To achieve monodispersity, these two stages must be separated and nucleation should be avoided during the period of growth.[17]

Methods for MNPs produced from vapor mainly include spray and laser pyrolysis. These two methods have been shown to be excellent techniques for the direct and continuous production of well-defined MNPs with high-production rate. The ultrafine particles are usually aggregated into larger particles by spray pyrolysis, while the ultrafine particles are less aggregated due to the shorter reaction time using laser pyrolysis.[18]

When the MNPs were prepared by the above-mentioned methods, another important issue is to maintain the stability of these particles without agglomeration or precipitation. For some pure materials or smaller size particles, it would be bound to instability towards oxidation in air. Therefore, it is necessary to develop efficient strategies to improve the chemical stability of MNPs. The most straightforward method seems to be protected by surface modification or assembly of MNPs. All these protection methods make the naked MNPs as a core and coated by a shell. The coating shell can roughly be divided into two major types: coating with surfactant and polymers, etc. organic shells or with silica, carbon, precious metals (such as Ag, Au) or oxides, etc. inorganic shells. All these shell materials can be modified on the surface of MNPs. Layer-by-layer (LBL) self-assembly is one of the most promising techniques to produce superparamagnetic composites. Using this strategy, the surface of MNPs can be coated with alternating layers of polyelectrolytes, nanoparticles, and proteins. Some other polymer-coated magnetite nanoparticles can be synthesized by microemulsion seed copolymerization in the presence of the magnetite nanoparticles. The particle size can be controlled by changing the monomer concentration and water/surfactant ratio.[19]

All in all, the small size and the modified agents render MNPs a potential candidate for their use in *in vivo* applications. Their preparation mainly involves three steps. First, the inorganic magnetic core is produced. Second, a stable biocompatible layer can be coated on the surface of the MNPs. Finally, the anchoring of the targeting moiety or a drug is necessary for molecular level applications.

2.2. Special features of magnetic nanoparticles

For ferromagnetic materials, the key parameters to determine magnetic properties such as coercivity (H_c) and susceptibility (χ) are composition, crystallographic structure, magnetic anisotropic energy, and vacancies and defects. For biomedical application, the important parameters may be mainly involved in superparamagnetism and surface effect.

2.2.1. Size and superparamagnetism

Biomedical applications like MR imaging, magnetic cell separation or magnetorelaxometry utilize the magnetic properties of the nanoparticles in magnetic fluids. These applications mainly depend on the hydrodynamic size and magnetic features of MNPs. When the MNPs are submicron moieties (between 1 nm–100 nm), they are different from those of bulk materials of the same composition. When the size is reduced to nanoscale, the magnetic and electronic properties, the role played by surface phenomena can make the NPs become excellent materials for biomedical applications (Fig. 1(a)).

It is well known that the large magnetic particles are multidomain structure. The domain wall, formed by the balance between the magnetostatic energy and the domain-wall energy, can separate the uniform magnetization. The magnetic anisotropic energy barrier from a spin-up state to spin-down state of the magnet is proportional to the product of the magnetic anisotropic constant and the volume of the magnet.[20] At tens of nanometers sizes, ferromagnetic MNPs become a single magnetic domain and therefore maintain one large magnetic moment. While bulk materials have magnetic anisotropic energies that are much larger than the thermal energy (k_b), the thermal energy of the nanoparticle is sufficient to readily invert the magnetic spin direction. Such magnetic fluctuation leads to a net magnetization of zero, and this behavior is called superparamagnetism (Fig. 1(b)).[21] The transition temperature from ferromagnetism to superparamagnetism is referred to as the blocking temperature (T_b) and is defined by Eq. (1):[22]

$$T_b = K_{eff}V/25k_b, \tag{1}$$

where T_b is the blocking temperature, K_{eff} refers to magnetic anisotropic constant and V is the volume of the magnet. The blocking temperature depends on the effective anisotropy constant, the size of the particles, the applied magnetic field, and the experimental measuring time. In a paramagnetic material, the thermal energy overcomes the coupling forces between neighboring atoms to cause random fluctuations in the magnetization direction, which results in a null overall magnetic moment. However, in superparamagnetic materials, the fluctuations affect the direction of magnetization of entire crystallites. The magnetic moments of individual crystallites compensate for each other and the overall magnetic moment becomes null. When an external magnetic field is applied, the magnetic moment of entire crystallites spontaneously aligns in the direction of a magnetic field. Unlike ferromagnetic substances and because of their size, superparamagnetic agents have no magnetic properties outside an external magnetic field.

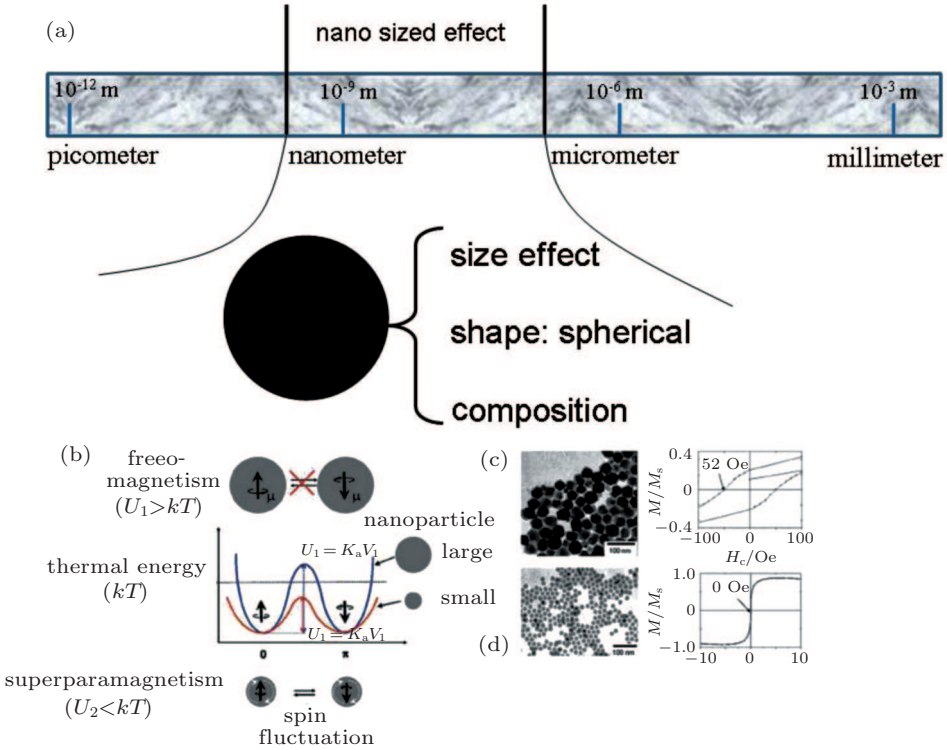


Fig. 1. Nanoscale transition of MNPs from ferromagnetism to superparamagnetism: (a) in nanometer scale, parameters such as size, shape, composition, and magnetocrystalline anisotropy strongly affect the coercivity, mass magnetization, and remanence of nanoparticles. (b) Energy diagram of MNPs with different magnetic spin alignments, showing ferromagnetism in a large particle and superparamagnetism in a small nanoparticle. (c) and (d) Size-dependent transition of iron oxide nanoparticles from superparamagnetism to ferromagnetism showing TEM images and hysteresis loops of (b) 55-nm and (c) 12-nm sized iron oxide nanoparticles. Panels (b), (c), and (d) reproduced with permission from Ref. [21]. The unit 1 Oe = 79.5775 A·m^{-1}.

The threshold diameter of SPIO MNPs typically lies in the range of a few tens of nanometers and depends on the nature of material. Fe-based NPs become superparamagnetic at sizes < 25 nm.[23] γ-Fe_2O_3 nanoparticles of 55 nm exhibit ferrimagnetic behavior with a coercivity of 52 Oe at 300 K, but smaller, 12-nm sized γ-Fe_2O_3 nanoparticles show superparamagnetism with no hysteresis behavior (Figs. 1(c) and 1(d)).[24] The critical single-domain size of Co nanoparticles is expected to be around 8 nm–10 nm. This superparamagnetic property enables the particles to maintain their colloidal stability and avoid aggregation when the external magnetic field is removed. Furthermore, the coupling interactions within these single magnetic domains result in much higher magnetic susceptibilities than paramagnetic materials. Such size-dependent mass magnetization values directly affect their MR signal enhancement capabilities for molecular imaging of biological targets.[25]

2.2.2. Surface effects

Surface coatings, assembly and the composites are an integral component of all MNP platforms for retaining the stability and biocompatibility. Normally, there are four aims to the surface modification and assembly for biomedical applications. First, the biocompatibility and toxicity of MNPs are criteria to take into account for their biomedical applications. For instance, the use of gold or silica as a shell material allows for potential application of toxic materials as nanoparticle cores with strong magnetic properties.[26] Secondly, although MNPs have superparamagnetic properties, surface charges on the MNPs are not adequate to prevent aggregation as a result of their high surface energy. Furthermore, upon intravenous injection, the surfaces of MNPs are subjected to adsorption of plasma protein, or opsonization. The conjugation of biocompatible polymers, such as dextran, PEG, or other protein resistant polymers, as surface coating, can prevent MNPs from aggregation and opsonization, thus can evade MNPs uptaken by the reticulo–endothelial system (RES), which increases plasma half-life in physiological solutions and blood circulation time.[27] Finally, the surface chemistry allows for the integration of functional ligands on the surface of MNPs, which enables MNPs to perform multiple functions simultaneously, such as in multimodal imaging, drug delivery, and real-time monitoring, as well as combined diagnostic and therapeutic approaches.

However, when the surface was modified by some biocompatibility materials, the coating or surface modification may negatively affect the magnetization due to quenching of surface effect. This reduction has been associated with different mechanisms, such as the existence of a magnetically dead layer on the particle's surface, the existence of canted spins, or the existence of a spin-glass-like behavior of the surface spins.[28] A clear correlation between the surface coating and the magnetic properties is not completely established. Hormes *et al.* discussed the influence of various coatings (e.g., Ag, Au) on the magnetic properties of cobalt nanoparticles, and came to the conclusion that a complex interplay between particle core and coating.[29] For example, a precious-metal layer around the MNPs will have a lower magnetic anisotropy than uncoated particles, whereas gold coating of iron particles enhances the anisotropy, an effect which has been attributed to alloy formation with the gold. Organic ligands, used to stabilize the MNPs, can also modify the anisotropy and magnetic moment of the metal atoms located at the surface of the particles by reducing the magnetic moment and a large anisotropy due to the quenching of the surface magnetic moments.[30]

2.3. Biomedical applications of magnetic nanoparticles

2.3.1. MRI contrast agents

The penetration of magnetic fields through human tissue and the ability to externally control magnetic materials have been investigated for use in medicine for centuries. One of the significant applications of these phenomena is MR imaging. As a non-invasive imaging modality, MR imaging can provide high resolution anatomical images. In an external magnetic field, the colloids of MNPs composed of crystals measuring 4 nm to 6 nm align and create very high local magnetic field gradients to induce water proton spin dephasing and consequently reducing the T_1 and T_2 relaxation times of the surrounding water. MNPs can generate a magnetic field in their vicinity. Such field inhomogeneity accelerates the phase decoherence of the spins. The efficiency by which a contrast agent can accelerate the proton relaxation rate in a homogeneous medium is called relaxivity of the agent and is defined by Eq. (2):[31]

$$R_{1,2} = R^0_{1,2} + r_{1,2}C, \tag{2}$$

where $R_{1,2}$ (s^{-1}) is the respective T_1 or T_2 proton relaxation rate in the presence of the contrast agent, $R^0_{1,2}$ are the relaxation rates in the absence of contrast agent and C is the contrast agent concentration (mM). The constant of proportionality $r_{1,2}$ ($s^{-1}\cdot mM^{-1}$) is called relaxivity and is a measure of how much the proton relaxation rate is increased per unit of concentration of contrast medium. In a first approximation, relaxivity varies as the square of the magnetic field induced in the vicinity of the water proton. The dipolar interaction between surrounding water protons and the high magnetic moment of superparamagnetic particles results in high longitudinal r_1 and transverse r_2 relaxivity. The theory describing the magnetic interac-

tion of superparamagnetic compounds with water protons has been described by different theoretical models derived from the classical outer sphere paramagnetic relaxation model.[32] In most situations, it is the significant capacity of superparamagnetic nanoparticles to increase the so-called T_2^* effect that is used in MR imaging. This T_2^* effect is called "susceptibility effect" and describes an increase of T_2^* relaxation rates due to a magnetization difference between different voxels in the MR imaging. A large magnetization difference occurs as a result of the non-homogeneous distribution of superparamagnetic particles, which gives rise to local field gradients that accelerate the loss of phase coherence of the spins contributing to the MR signal. This process is much more important for superparamagnetic particles than for paramagnetic species, as the induced magnetization of a superparamagnetic particle is high due to the high susceptibility of iron oxide. The magnitude of this susceptibility effect depends on many factors, such as compartmentalization of the contrast agent, type of imaging sequence, aggregation of the contrast agent. It should be noted that any aggregation has an important impact on the T_1, T_2 or T_2* efficiency of a superparamagnetic particle. At the clinical field used in MRI (1 T to 3 T), agglomeration tends to slightly decrease r_1 but markedly increases r_2.[33]

2.3.2. Drug delivery and therapeutic functions

The regularly employed superparamagnetic nanoparticles in drug delivery consist of NPs, nanospheres, liposomes, and microspheres. In these systems, the drugs are bound to the NPs' surface or encapsulated in magnetic liposomes and microspheres. The physical principles underlying magnetic targeting therapy are derived from the magnetic force exerted on MNPs by a magnetic field gradient, as in Eq. (3):[34]

$$Fm = Vm\Delta\chi\nabla\left(\frac{1}{2}B\cdot H\right), \tag{3}$$

in which the magnetic force is related to the differential of the magnetostatic field energy density, $(1/2)B\cdot H$. Thus, if $\Delta\chi > 0$, the magnetic force acts in the direction of steepest ascent of the energy density scalar field. According to the basis of MNPs' properties, the biological effects can be divided into thermal and non-thermal effects. Figure 2 is a schematic illustration of MNPs and their composites to realize the drug delivery and therapeutic functions. For drug delivery, the effectiveness of the therapy depends on several physical parameters, including the field strength, gradient and volumetric and magnetic properties of the MNPs. As the delivery carriers are normally administered intravenously, hydrodynamic parameters such as blood flow rate, ferrofluid concentration, infusion route, and circulation time also will play a major role.[35]

In terms of magnetization value, coercivity, and anisotropy, the nanoparticle's heat induction properties have also attracted significant interest these days for magnetic hyperthermia therapy.[36] In this process, the internal magnetic spins of nanoparticles relax in phase and continuously upon application of an alternating magnetic field of 100 kHz–1000 kHz as a consequence of a combination of Néel and Brown processes. While the spins relax, energy associated with transitions between the up and down spin states is emitted as heat.[37] Because magnetic fields are not significantly attenuated upon transmission through biological tissues, they can be utilized for hyperthermia therapy of deeply buried tumors. Moreover, cancer cells (temperature initiating apoptosis of cancer cells at 42 °C–45 °C) are usually more sensitive to heat than benign cells, which is sufficient to provide the temperature range for cancer cell apoptosis.[38] Heat induction from the MNPs is proportional to the size, magnetization value, and magnetic anisotropy of nanoparticles, concentrations in tissues, intensity, and frequency of alternating magnetic field.

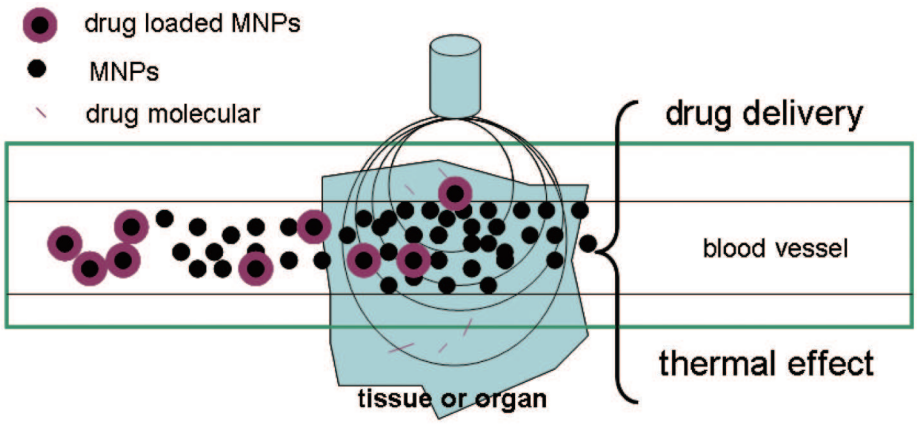


Fig. 2. Schematic diagram of MNPs and their composites in hypothetical magnetic drug delivery system: the magnetic field gradient can capture magnetic carriers flowing in the circulatory system. Then MNPs can release the loaded drugs into the specific tissue or organ. The aggregation of MNPs can also produce thermal effect to treat disease.

2.4. Ultrasonic characteristics of magnetic nanoparticles liquid

When an external magnetic field is applied to magnetic and MR fluids, some of the inner particles coagulate and form a clustering structure. Several theoretical and experimental studies have been conducted to investigate the influences of the ultrasonic propagation during the formation of clustering structures. The results show that the ultrasonic propagation velocities in magnetic and MR fluids change according to the magnetic field intensity, interval time, the temperature, and angle of magnetic field. Ultrasonic propagation velocity changes when the magnetic field is applied. The change in ultrasonic propagation velocity is evaluated by Eq. (4):[39,40]

$$\Delta V/V_0 = \frac{V - V_0}{V_0}, \tag{4}$$

where V and V_0 are ultrasonic propagation velocities with and without an external magnetic field, respectively. Under a uniform external magnetic field, a remarkable level of anisotropy is observed, generally proving that the clusters form along the direction of the magnetic field. After removal of the magnetic field, a few clusters still remain due to a residual magnetic field effect proportional to the strength of the magnetic field. These results seem to be related to Brownian motion, residual magnetic field, and clustering of the magnetic particles under an external magnetic field.[41,42]

From the point of biomedical applications, acoustical properties of MR fluid may be easily changed by applying magnetic fields. An active matching layer could be an interesting example or any coating whose attenuation might be changed depending on the requirements. This study is also beneficial for understanding physical properties of magnetic MBs.

3. Microbubble formalism and acoustic characteristics

3.1. Design and preparation of microbubbles

Initially, the MBs that formed during the injection of dye or saline were clearly effective for ultrasound contrast enhancement. However, air bubbles dissolve very rapidly owing to the high surface tension at the gas–air interface. They are very short-lived and difficult to reproduce consistently. Some reports demonstrated that a 10-μm unencapsulated air bubble dissolves in 1.17 s and in 6.63 s in degassed and in air-saturated water solutions respectively.[43] Therefore MBs encapsulated with a solid shell to stabilize the gas–liquid interface were introduced. The shell is made from lipid, surfactant, protein or biodegradable polymer. Simultaneously, low diffusivity gases were introduced to further increase the microbubble circulation time. These encapsulated shell of MBs can diminish surface tension and make MBs stable enough to sustain the pressures exerted within the vasculature. The stabilized MBs now are being employed for several biomedical applications, including contrast-enhanced ultrasound, drug, and gene delivery and metabolic gas delivery.

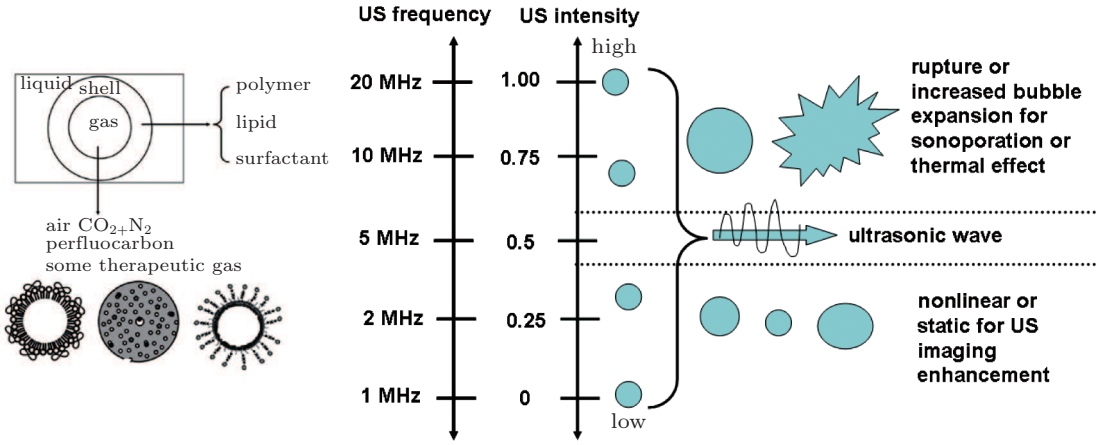


Fig. 3. The schematic diagram of MBs' structure and loading strategies of drugs, genes, and targeting peptide. At low US intensity, the MBs oscillate in a nonlinear fashion with minimal destruction, which can be used to enhance the US imaging. As the acoustic power increase, the bubbles cannot compress and make the bubbles unstable until reaching a point of rupture, which can be viewed as the basis for therapeutic ultrasound.

In order to control the size, composition, stability, and uniformity of MBs and give MBs better diagnostic and therapeutic properties, advanced preparation techniques are required. Nowadays, these methods are mainly divided into four classes. One is that the flowing liquid is used to create the MBs. The second type is to blow only gas to generate MBs. The third type is used to prepare the polymer encapsulated MBs, which includes emulsion solvent vaporization,

cross linking polymerization, etc. And the final type is to use much less power to produce MBs including flow focusing, microchannel, etc. Conventional processing techniques such as sonication and high shear emulsification offer high yield and low cost production, but poor control over size and uniformity. In light of the improvements in microbubble uniformity, more processing methods such as ink jet printing, electrohydrodynamic atomisation, and microfluidic processing techniques were developed. These novel processing techniques enable gas-filled MBs to be prepared in a single step with a predetermined mean diameter and narrow size distribution. After producing multi-layered coated bubbles, the nanoparticles or specific protein ligands can also be attached on the surface of MBs electrostatically or by chemical reaction.[44] The detailed information about the MBs generation can be found in Ref. [45]. Figure 3 is the simple explanation of the MBs' structure and their biological effects.

3.2. Actions of MBs with ultrasound waves

MBs are more compressible than soft tissue. When MBs are exposed to an oscillating acoustic signal, alternate expansion and contraction occurs. However, because MBs do not remain static in the presence of an ultrasound wave, the interactions of MBs with an ultrasound beam are complex besides the simple compressibility and the density.

3.2.1. Enhancement of ultrasound imaging by means of MBs

Based on the principle of scattering and reflection exploited by ultrasound imaging, an ultrasound contrast agent material has to possess a high scattering cross section in order to provide a significant scatter enhancement compared to the surrounding tissue. The scattering cross section σ for a linear scatterer that is much smaller than the incident ultrasound pulse wavelength is given by Eq. (5):[46]

$$\sigma = \left(\frac{4}{9}\pi R^2 (kR)^4\right)\left(\left(\frac{\kappa_s - \kappa}{\kappa}\right)^2 + \frac{1}{3}\left(\frac{3(\rho_s - \rho)}{2\rho_s - \rho}\right)\right)^2, \quad (5)$$

where R is the radius of the scatterer ($\ll \lambda$), λ is the wavelength, $k = 2\pi/\lambda$ is the wave number, κ_s is the compressibility of the scatterer, κ is the compressibility of the surrounding medium, ρ_s is the density of the scatterer, and ρ is the density of the surrounding medium. As ultrasound imaging exploits changes in compressibility and density, it can be calculated from Eq. (5) that the use of gas MBs ensures maximum cross section.

At low acoustic power (< 50 kPa), the MBs oscillate linearly, and the echo is mainly fundamental; when the acoustic pressure increases (50 kPa–200 kPa), nonlinear oscillations occur, giving rise to harmonics and subharmonics shown in Fig. 4.[47] Every echo component can be detected for construction and imaging. According to the different components detected by the detection procedure, the detection procedures of MBs can be classified as fundamental imaging, harmonic imaging, and subharmonic imaging. Recently, second harmonic imaging is one of the most commonly used imaging modality in clinic and most of the high-end B-mode ultrasound imaging systems have the function of second harmonic imaging.[48,49] Destruction of MBs has been observed at much higher powers during ultrasonic excitation. The mechanisms of destruction include the outward diffusion of the gas during the compression phase, diffusion from large shell defects, and from complete fragmentation of MBs. Microbubble destruction during high-power ultrasound exposure is an important feature for both perfusion imaging protocols and for therapeutic applications for local delivery of drug or gene payload.[50]

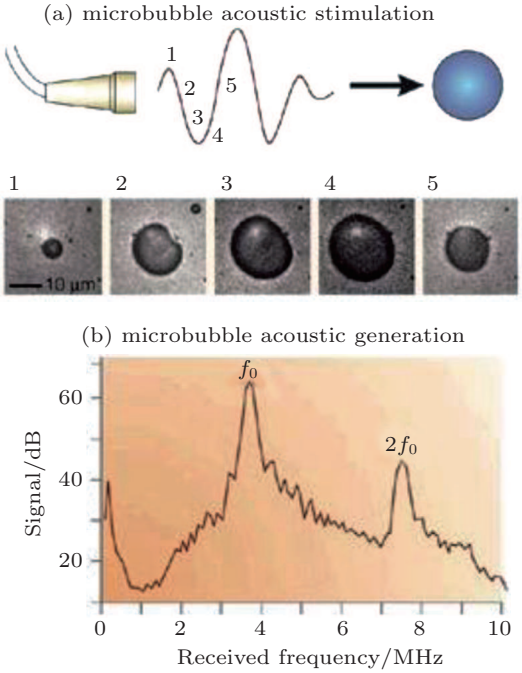


Fig. 4. Schematic plot of the acoustic properties of MBs. The microscopy images demonstrate volumetric oscillation of a microbubble during exposure to ultrasound. Frequency versus amplitude data from MBs demonstrating returning signal both at the fundamental (f_0) and second harmonic ($2f_0$) frequencies.[46]

3.2.2. Ultrasound-assisted drug delivery of MBs

In recent years, therapeutic applications of ultrasound have gained new interest as a result of their exploitation for drug or gene delivery. Depending on the energy delivered by ultrasound, either thermal or non-thermal effects can be produced. Each has its own application. With each ultrasonic cycle under high ultrasound intensities, a fraction of the energy in the propagating wave is absorbed by tissue to induce local heating. The rate of absorption is tissue-dependent

and increases with the increasing ultrasound frequency. These thermal effects can locally ablate tissue. This property is employed in high-intensity focused ultrasound (HIFU) surgery or ultrasound-based physiotherapy.[51] With low ultrasound intensities, there is no significant biological effect due to temperature increases less than or equal to 1 °C. The non-thermal effect can happen at low ultrasound intensities. Cavitation, mechanical streaming, and radiation forces are the main non-thermal effects mechanism. Especially, the cavitation-related mechanisms include radiation force, microstreaming, shock waves, free radicals, microjets, and strain. These effects can induce some benefits such as tissue healing or ultrasound-mediated delivery. Because the MBs can reduce the threshold of energy needed for cavitation, US can trigger the controlled release of a drug, gene encapsulated in MBs or in their surrounding in a non-invasive manner.[52]

4. Magnetic and acoustic character of magnetic microbubbles (MMBs)

4.1. Fabrication of magnetic microbubbles

Recently, functionalized MBs embedding nanoparticles or quantum dots in their shells have been developed for emerging applications in the biological, medical, and materials sciences.[53] The encapsulation of paramagnetic MR imaging nanoparticles into the shell structure could facilitate a potential application as bimodal contrast agents for echosonography, MR imaging, and for targeted drug delivery. The MNPs can be embedded in the solid polymers shells. Softer vehicles, like lipid materials, have also been developed to contain the nanoparticle cargo, which is enclosed within a self-assembled phospholipid or polymer film for the nanoparticle loading (Fig. 5(a)).[54] It is interesting to understand the interaction mechanism among magnetic MBs, the magnetic field, and the ultrasonic field. It was important to investigate their echogenicity and also their ability to be magnetically retained under flow (Fig. 5(b)).

The MNPs can be loaded in the inner or outer side of the shell MBs. There are mainly two methods to load the MNPs in the shell of MBs. One is physical, another is chemical reaction.[55] By electrostatical methods, Soetanto *et al.* attached magnetic microparticles to the microbubble surface coated with charged stearates.[56] Our group had also developed PLA–PVA double-layered polymeric MBs with the encapsulation of superparamagnetic iron-oxide (Fe_3O_4, SPIO) nanoparticles in the bubble shell by the multiple emulsion methods.[57,58] The SPIO γ-Fe_2O_3 nanoparticles also can be coated on the surface of the EDC chemical reaction.[59]

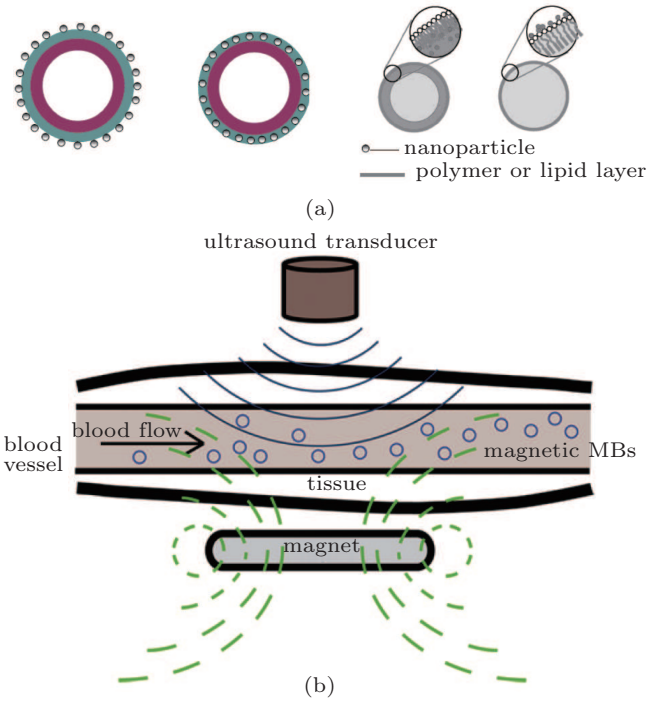


Fig. 5. (a) Schematic diagram of the types of the MNPs embedded in the shell of the MBs. (b) Schematic plot of the ultrasound flow: When magnetic MB suspension is injected into the blood vessel and dual modal images obtained using an ultrasound and MR imaging probe. At the same time, the magnetic MBs can be controlled by both ultrasonic and magnetic field.

4.2. Acoustic response of magnetic microbubbles

In the absence of any particles on its surface, a bubble would be expected to exhibit symmetrical radial oscillations in response to a low-intensity ultrasound field. The presence of particles on the shell of MBs, however, prevents the bubble from expanding and contracting with equal amplitude, due to the packing together of the particles during compression. Therefore, it must be considered that the high echogenicity characteristic of MBs can be reduced when MNPs decorated on the surface of MBs. Stimulated by the challenging study, our group aims to study the influence of the nanoparticle embedded shell on the microbubble scattering property. Based on the bubble dynamics theory,[60,61] the shell properties of the samples (MBs with different amount of Fe_3O_4 nanoparticles in the shells and 2 μm in average radius) are estimated using an optimization method. Then, given the excitation frequency of 3.5 MHz, the scattering cross sections of the samples are calculated with the estimated shell viscoelastic parameters (χ and κ_s). Acoustic scattering, defined as the acoustic power scattered in all directions per unit incident intensity, is given by scattering cross section $\sigma_s(\omega)$, which can be estimated as Eq. (6):[62]

$$\sigma_s(\omega) = 4\pi R_0^2 \frac{\Omega^4}{(\Omega^2-1)^2+\Omega^2\delta^2}, \quad \Omega = \frac{\omega}{\omega_0}. \tag{6}$$

According to Eq. (6), when the bubble's initial radius R_0

and the excitation frequency are set, the scattering cross section $\sigma_s(\omega)$ is determined by the resonance frequency ω_0 and the damping coefficient. The resonance frequency ω_0 is relative to the shell elasticity parameter, and the damping coefficient is relative to the shell viscosity parameter ω_s. Thus, by calculating the shell viscoelastic properties, we can obtain the information about the influence on acoustic scattering. Several parameters such as microbubble concentration, microbubble size, excitation frequency, and shell viscoelastic properties together determine the scattering response. Compared with magnetic MBs and MBs without MNPs, the scattering properties are all the same except for the shell properties. It is found that when the MNPs inclusion concentration increases, the scattering cross section of MMBs increases at first and then decreases (Fig. 6(a)). Therefore, controlling the appropriated concentration of MNPs in the shell of microbubble is beneficial for the MMBs in the biomedical imaging applications.

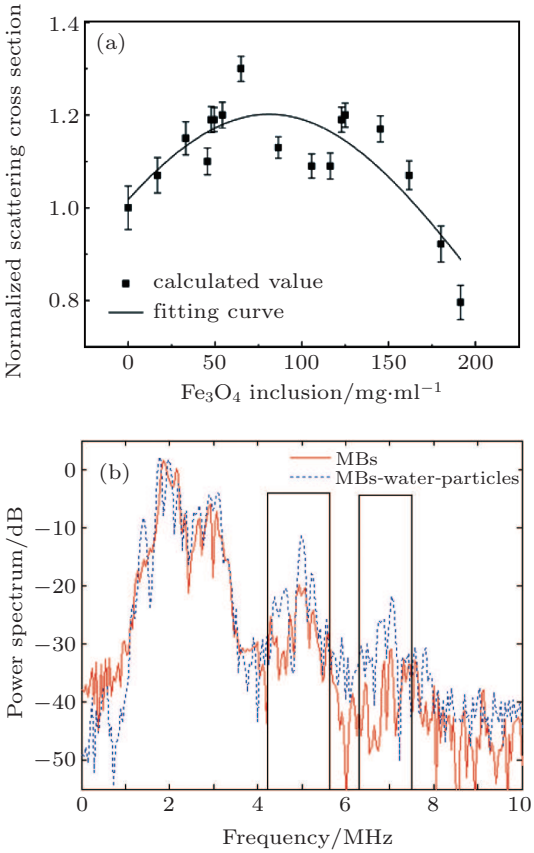


Fig. 6. (a) The calculated scattering cross sections of the MMBs with the different MNPs concentration. (b) The backscattered RF signals from MBs and MBs-water-particle.

Result in Fig. 6(b) shows that amplitudes of second and third harmonic for the MBs-water-MNPs (Fe_2O_3) are highest. The reason may be that the deposition of nanoparticles on the surface of the microbubble alters the shell's viscoelastic property and affects the microbubble's behavior. And the uneven distributed nanoparticles result in asymmetrical oscillation. All of them are responsible for the increase of the nonlinear behavior of MBs. Moreover, nanoparticle alters the vibration property of the microbubble and enhances the nonlinear properties of backscatter, which is potentially suitable for the medical ultrasound contrast harmonic imaging. Thus the magnetic MBs with the higher nonlinearity can be beneficial for improving the contrast effect of ultrasound harmonic imaging.

4.3. Magnetic response of magnetic microbubbles

When a microbubble is placed in a fluid with a magnetic permeability in which an external uniform magnetic field H_0 is present, the field around the microbubble is disturbed. One of the ways to change the magnetic susceptibility of MBs in the medium is to change the susceptibility of the encapsulated gas. If the susceptibility of the gas filled in MBs differs from that of the surrounding medium, MBs create localized perturbations in the magnetic field, thereby acting as "susceptibility contrast agents" and shortening T_2 and T_2*. The effects depend on magnetic field strength and are much greater at higher field strength.[63,64] Some experiments showed that the MBs can be used as MR susceptibility contrast agents on a 2-T and 4.7-T MR scanner.[65,66]

On the other hand, based on the principle that the rate constant for relaxation of the MR signal (R_2) from a solution containing spheres is related to the size of the sphere, when the distensible MBs are present in a pressure-varying medium, the changes in size due to changes in pressure (P) cause changes in signal decay rate constants $1/T_2$ (or R_2) and $1/T_2^*$ (or R_2^*). The susceptibility of air MBs was measured by transverse relaxation increase (R_2^*). The time course of the transverse relaxation increase $R_2^*(t)$ was estimated as Eq. (7):[67]

$$R_2^*(t) = -\ln(S(t)/S_f)/TE, \tag{7}$$

where S_f is the final signal intensity. The R_2^* is to be proportional to the MBs volume fraction. The volume change of the MBs resulting from the oscillation can change the transverse relaxation rate. From Fig. 7, it is clear that the increase of MBs' volume is equivalent to increasing the susceptibility difference between the bubble and its environment. Based on this principle, some researches have reported that on a 4.7-T and 7-T MR scanner, MBs coated with shells of liposomes or human albumin have shown great potential application as MR pressure sensors based on pressure-induced susceptibility change *in vitro* and *in vivo*. The *in vitro* and *in vivo* MRI experiments all show that the MBs can be fabricated to be the effective MR susceptibility contrast agents. However, although the above-mentioned studies indicated the good magnetic response about MBs, all studies were performed with high-field

MR systems because MBs have a relatively weaker susceptibility effect. In practice, one means of enhancing the susceptibility is by coating or embedding magnetically active particles of high magnetic dipole moment on the lipid shells of gas-containing microbubbles. In order to obtain a significant increase in $\Delta\chi_{\text{eff}}$, thousands of magnetically active particles need to be embedded on the microbubble shell.[68,69] At this condition, large magnetic susceptibility comes from SPIO particles. For *in vitro* measurement, the measured transverse relaxation rate (R_2) of the samples may be described by Eq. (8):

$$R_2^{\text{Total}} = R_2^{\text{MBs}} + R_2^{\text{MNPs}}. \tag{8}$$

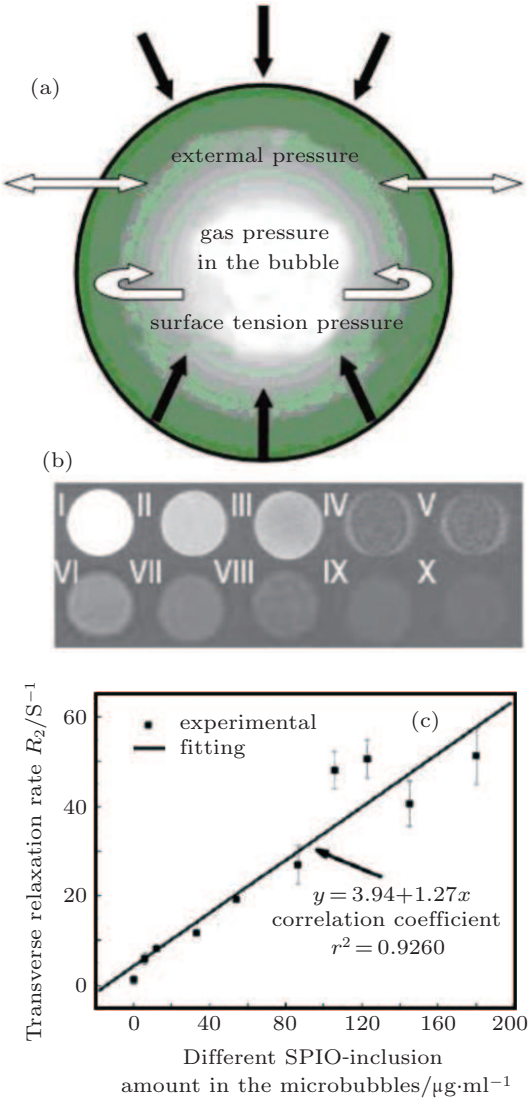


Fig. 7. Schematic plot of the size change according to the pressures (a). (b) The *in vitro* MRI images using 7-T scanner. I: de-ionized water, II: EMBs without SPIO inclusion, SPIO-inclusion EMBs with different SPIO concentrations (III–X are 5.73, 12.06, 33.14, 54.23, 86.47, 105.69, 122.85, 145.24, 180.23 mg/ml respectively). After the corresponding T_2 computed from the T_2-maps were obtained. The relationship of R_2 versus SPIO inclusion (mg/ml) is shown in panel (c). The linear fit was obtained between the SPIO-inclusion concentration in the MBs and the transverse relaxation rate (R_2). From this curve, it is found that the effect of increasing total magnetic nanoparticle density in the shell is related to increasing the susceptibility effects of the MBs.

We examine the possibility of enhancing the effective magnetic susceptibility difference by embedding the different concentrations 12-nm Fe_3O_4 in the shell. The overall transverse relaxation rate R_2^{Total} is considered as the sum of that contributed by MBs, R_2 bubble, and that contributed by SPIO particles, R_2^{SPIO}. Generally speaking, $R_2^{\text{SPIO}} \gg R_2^{\text{bubble}}$, therefore R_2^{SPIO} contributed by SPIO Fe_3O_4 nanoparticles embedded in MBs is greater than that contributed by the free SPIO Fe_3O_4 nanoparticles in the solution of the same concentration when volume fraction is greater than 60% (Fig. 7(c)). MBs can hold the nanoparticles in the shells and make numbers of MNPs localized and concentrated per volume inside the shell, thus the number of MNPs per volume much higher than those anywhere for the free MNPs case. Since in this case the effect due to highly concentrated MNPs dominates, the linear relationship condition with respect to $\Delta\chi$ based on the uniformly distributed MBs' susceptibility effect is no longer valid. In fact, the effect of adding the number of SPIO per volume becomes quite nonlinear.[70] There is a strong dependence on the type of magnetically active agents, the nanoparticle radius, the magnetic saturation or total magnetic susceptibility, and the distribution in the shell.

5. Applications of magnetic microbubbles in biomedicine

5.1. Multimodal imaging of MMBs

Initially, the motivation and objectives of designing magnetic microbubbles are to combine MBs and MNPs. Therefore, the introduction of nanoparticle onto the surface of microbubble produces a useful tool for multi-mode imaging and multifunctional contrast agent. For example, our group engineered double-layered SPIO-encapsulated MBs which showed improved r_2 relaxivity and better contrast enhancement than SPIO free MBs or SPIO-included MBs on the surface. When the MNPs embedded in the shell of MBs, the high echogenicity, characteristic of MBs coated with a thin self-assembled film of small molecules, is not reduced by the grafting of MNPs. The *in vitro* MRI experiments revealed a gradient decrease of gray scale associated with a corresponding increase of the SPIO concentrations. And the transverse relaxation fitted well to a linear relationship with different SPIO-inclusion amounts in the MBs. Then *in vitro* ultrasound imaging was performed to observe a distinct "brightening" contrast enhancement in the region of interest (ROI) with a certain MMBs concentration. After the injection of MMBs into the livers of living rats, real-time MRI anatomical images revealed a clear negatively enhanced contrast. Later, Liu *et al.* also reported that poly(butyl cyanoacrylate) (PBCA) polymer en-

capsulated ultrasmall superparamagnetic iron-oxide (USPIO) nanoparticles exhibited strong contrast in US and an increased transversal relaxation rate in MR.[71,72] Although these existing findings reveal a promising ultrasound-MRI dual modal imaging modality in medical applications, future efforts in this regard will focus on the coupling of antibodies or peptides to the microbubble surface, to make them useful for multi-modal molecular imaging.

5.2. Ultrasound assisted drug delivery of MMBs

In addition to providing contrast enhancement in ultrasound imaging, to utilize microbubble-nanoparticle hybrid vehicles for drug release and therapy is another promising strategy for medical treatment applications. The basic mechanism of MBs for delivery vesicle mainly based on enhanced membrane transport, changes in tissue/vascular transport properties, and mechanical or thermal changes. Acoustic cavitation induces high fluid velocities, shear forces, and local temperature increases, thus producing biological effects and altered transport kinetics near the site.[73,74] Combination of MBs with nanoparticles into one single delivery system can also facilitate the possibility of effective drug transport from extracellular microenvironment to cell membrane, and controllable release at the diseased sites.[75] In the study, we have demonstrated that it is possible to control the release of Fe_3O_4 NPs from shells of embedded microbubbles into cells by ultrasonic excitation. Consequently, those Fe_3O_4-NP-labeled cells can be noninvasively tracked by MRI. The appropriate balance between generation of suitable cell porosity for drug delivery and, simultaneously, maintenance of the integrity of the plasma membrane could be achieved by adjusting the acoustic intensity of the applied US, which would provide medical professionals with an alternative way to deliver nanoparticles into targeted cells noninvasively and effectively.[76] However, the multiple-scale interactions of magnetic MBs are rather complicated and warrant further research.

5.3. Magnetic field-controlled drug delivery and release of MMBs

An alternative and potentially complementary strategy is to use MBs loaded with MNPs whose location can be manipulated using an externally applied magnetic field. Enhanced transfection has been demonstrated *in vitro* and *in vivo*. As mentioned above, it was hypothesized that the increased transfection rates were due to the increase in both concentration and proximity of the MBs to the target cells produced by the magnetic field. Further investigation to fully understand the mechanisms of enhancement and optimization of the delivery protocols is required. One question which was not addressed in the studies is whether the MNPs significantly affected the behavior of the MBs in the presence external magnetic field. In order to determine the influence of these factors on a range of microbubble characteristics, their dynamics and magnetics have been investigated in *in vitro* and *in vivo* studies.[77] A recent paper reported that magnetic MBs were used for gene delivery to Chinese hamster ovary cells. Different formulations of magnetic MBs, non-magnetic MBs, and magnetic liquid droplets were co-injected with naked plasmid DNA encoding for luciferase and the cells exposed to a magnetic field, ultrasound or both. In addition, the experiments were performed with the cells on either the upper or lower surface of the culture plate so that in the case of the former, buoyant bubbles would be in contact with the cells. The results show that they would be separated by a distance of 2 mm unless they were magnetically-responsive in which case they would be translated downwards in the presence of a magnet. It was found that the highest rates of transfection were achieved with simultaneous exposure to ultrasound and a magnetic field.[78]

6. Summary and perspectives

In the field of disease-specific imaging, MR and US imagings are widely used modalities for various experimental and clinical applications. It is essential to develop a multimodal co-constructed platform for multi-functional biomedical applications. Magnetic MBs have been developed as a new multifunctional delivery system. The magnetic shelled bubbles can possess sufficient magnetization such that they can be controlled with conventional magnets, and their shell elasticity still allows for volume oscillations in moderate acoustic fields. Since maintaining the magnetic and acoustic characteristics, the magnetic MBs can be visualized using ultrasound imaging, magnetic resonance imaging, and can be localized by using an externally applied magnetic and ultrasonic field. Further, the MMBs exploit the combined effects of magnetofection and sonoporation for therapeutic delivery. However, MMBs is the co-constructed multiscale platform from magnetics and acoustics. The mechanism should be further studied. And by coupling a targeting-ligand to surface of the MMB, such as a monoclonal antibody, it will be possible to target the MMB to specific tissues within a subject. To realize the molecular imaging and accurate drug delivery will be the future promising and interesting investigations.

References

[1] Mahmoudi M, Sant S, Wang B, Laurent S and Sen T 2011 *Adv. Drug Deliver. Rev.* **63** 24

[2] Ferrara K, Pollard R and Borden M 2007 *Ann. Rev. Biomed. Eng.* **9** 415

[3] Unger E C, Hersh E, Vannan M, Matsunaga T O and McCreery T 2001 *Prog. Cardiovasc. Dis.* **44** 45
[4] Stride E and Saffari N 2003 *Proc. Inst. Mech. Eng.* **217** 429
[5] Ohelerth S and O'Brien R T 2007 *Vet. J.* **174** 501
[6] Alexander A L, McCreery T T, Barrette T R, Gmitro A F and Unger E 1996 *Magn. Reson. Med.* **35** 801
[7] Sun C, Lee J S H and Zhang M 2008 *Adv. Drug Deliver. Rev.* **60** 1252
[8] Jabr-Milane L, van Vlerken L, Devalapally H, Shenoy D, Komareddy S, Bhavsar M and Amijia M 2008 *J. Control Release* **130** 121
[9] Chen Z P, Zhang Y, Zhang S, Xia J G, Liu J W, Xu K and Gu N 2008 *Colloid Surface A* **316** 210
[10] Sukhorukov G B and Möhwald H 2007 *Trends Biotechnol.* **25** 93
[11] Yallapu M M, Othman S F, Curtis E T, Gupta B K, Jaggi M and Chauhan S C 2011 *Biomaterials* **32** 1890
[12] Louie A 2010 *Chem. Rev.* **110** 3146
[13] Gao J, Gu H and Xu B 2009 *Accounts Chem. Res.* **42** 1097
[14] Sun C, Lee J S and Zhang M 2008 *Adv. Drug Deliver. Rev.* **60** 1252
[15] Pankhurst Q A, Connolly J, Jones S K and Dobson J 2003 *J. Phys. D: Appl. Phys.* **36** R167
[16] Pedro T, del Puerto M, Veintemillas-Verdaguer S, Gonzalez-Carreńo T and Serna C J 2003 *J. Phys. D: Appl. Phys.* **36** R182
[17] Willis A L, Turro N J and Obrien S 2005 *Chem. Mater.* **17** 5970
[18] Xia B, Lenggoro I W and Okuyama K 2001 *Adv. Mater.* **13** 1579
[19] Liu J, Zhang Y, Yan C, Wang C, Xu R and Gu N 2010 *Langmuir* **26** 19066
[20] Corot C, Robert P, Idee J M and Port M 2006 *Adv. Drug Deliver. Rev.* **58** 1471
[21] Jun Y W, Seo J W and Cheon J 2008 *Accounts Chem. Res.* **41** 179
[22] Lee J, Isobe T and Senna M 1996 *J. Colloid Interface Sci.* **177** 490
[23] Cheon J, Kang N J, Lee S M, Yoon J H and Oh S J 2004 *J. Am. Chem. Soc.* **126** 1950
[24] Morales M P, Veintemillas-Verdaguer S, Montero M I and Serna C J 1999 *Chem. Mater.* **11** 3058
[25] Berry C C and Curtis A S G 2003 *J. Phys. D: Appl. Phys.* **36** R198
[26] Ge Y, Zhang Y, He S, Nie F, Teng G and Gu N 2009 *Nanoscale Res. Lett.* **4** 287
[27] Lacroix L M, Delpech F, Nayral C, Lachaize S and Chaudret B 2013 *Interface Focus* **3** 20120103
[28] Derfus A M, von Maltzahn G, Harris T J, Duza T, Vecchio K S, Ruoslahti E and Bhatia S N 2007 *Adv. Mater.* **19** 3932
[29] Lu A H, Salabas E L and Schüth F 2007 *Angew. Chem. Int. Ed.* **46** 1222
[30] Zeng H and Sun S 2008 *Adv. Funct. Mater.* **18** 391
[31] Sun S H 2006 *Adv. Mater.* **18** 393
[32] Park J, Joo J, Kwon S G, Jang Y and Hyeon T 2007 *Angew. Chem., Int. Ed.* **46** 4630
[33] Mahmoudi M, Sant S, Wang B, Laurent and Sen T 2011 *Adv. Drug Deliver. Rev.* **63** 24
[34] Dobson J. 2006 *Drug Dev. Res.* **67** 55
[35] Ferrari M 2005 *Nat. Rev. Cancer* **5** 161
[36] Hergt R, Dutz S, Muller R and Zeisberger M 2006 *J. Phys.: Condens. Matter* **18** 2919
[37] Noh S H, Na W, Jang J T, Lee J H, Lee E J, Moon S H, Lim Y, Shin J S and Cheon J 2012 *Nano Lett.* **12** 3716
[38] Riegler J, Allain B, Cook R J, Lythgoe M F and Pankhurst Q A 2011 *J. Phys. D: Appl. Phys.* **44** 055001
[39] Bramantya M A, Motozawa M, Takuma H, Faiz M and Sawada T 2009 *J. Phys.: Conf. Ser.* **149** 012040
[40] Sawada T, Nishiyama H and Tabata T 2002 *J. Magn. Magn. Mater.* **252** 186
[41] Rodríguez-López J, Segura L E and de Espinosa Freijo F M 2012 *J. Magn. Magn. Mater.* **324** 222
[42] Sboros V 2008 *Adv. Drug Deliver. Rev.* **60** 1117
[43] Stride E and Edirisinghe M 2008 *Soft Matter* **4** 2350
[44] De Jong N, Cornet R and Lancee C T 1994 *Ultrasonics* **32** 447
[45] Parmar R and Majumder S K 2013 *Chem. Eng. Process.* **64** 79
[46] Lindner J R 2004 *Nat. Rev Drug Discov.* **3** 527
[47] Leong-Poi H, Song J, Rim S, Christiansen J, Kaul S and Lindner J R 2002 *J. Am. Soc. Echocardiog.* **15** 1269
[48] Raisinghani A and DeMaria A N 2002 *Am. J. Cardiol.* **90** 3J
[49] Miller D L, Averkiou M A, Brayman A A, Everbach E C, Holland C K, Wible J H and Wu J 2008 *J. Ultrasound Med.* **27** 611
[50] Basude R and Wheatley M A 2001 *Ultrasonics* **39** 437
[51] Chomas J E, Dayton P, Allen J, Morgan K and Ferrara K W 2001 *IEEE Trans. Ultrason. Ferr. Freq. Control* **48** 232
[52] O'Brien W D 2007 *Prog. Biophys. Mol. Bio.* **93** 212
[53] Ferrara K W 2008 *Adv. Drug Deliver. Rev.* **60** 1097
[54] Nguyen P N, Nikolova G, Polavarapu P, Waton G, Phuoc L T, Pourroy G and Krafft M P 2013 *RSC Advances* **3** 7743
[55] Zhao X, Quinto-Su P A and Ohl C D 2009 *Phys. Rev. Lett.* **102** 024501
[56] Schmidt W and Roessling G. 2006 *Chem. Eng. Sci.* **61** 4973
[57] Soetanto K and Watarai H 2000 *Jpn. J. Appl. Phys.* **39** 3230
[58] Yang F, Li L, Li Y, Chen Z, Wu J and Gu N 2008 *Phys. Med. Biol.* **53** 6129
[59] Yang F, Li Y, Chen Z, Zhang Y, Wu J and Gu N 2009 *Biomaterials* **30** 3882
[60] He W, Yang F, Wu Y, Wen S, Chen P, Zhang Y and Gu N 2012 *Mater. Lett.* **68** 64
[61] Alexander A L, McCreery T T, Barrette T R, Gmitro A F and Unger E C 1996 *Magn. Reson. Med.* **35** 801
[62] Pisani E, Tsapis N, Galaz B, Santin M, Berti R, Taulier N, Kurtisovski E, Lucidarme O, Ourevitch M, Doan B T, Beloeil J C, Gillet B, Urbach W, Bridal S L and Fattal E 2008 *Adv. Funct. Mater.* **18** 2963
[63] Dharmakumar R, Plewes D B and Wright G A 2005 *Phys. Med. Biol.* **50** 4745
[64] Lakes R S, Kose S and Bahia H 2002 *J. Eng. Mater. Technol.* **124** 174
[65] Schenck J F 1996 *Med. Phys.* **23** 815
[66] Zhao L and Albert M S 1998 *Nucl. Instrum. Methods Phys. Res. A* **402** 454
[67] Wong K K, Huang I, Kim Y R, Tang H, Yang E S, Kwong K K and Wu E X 2004 *Magn. Reson. Med.* **52** 445
[68] Yang F, Li Y, Chen Z, Zhang Y, Wu J and Gu N 2009 *Biomaterials* **30** 3882
[69] Ueguchi T, Tanaka Y, Hamada S, Kawamoto R, Ogata Y, Matsumoto M, Nakamura H and Johkoh T 2006 *Magn. Reson. Med. Sci.* **5** 147
[70] van Beek E J, Wild J M, Kauczor H U, Schreiber W, Mugler J P III and de Lange E E 2004 *J. Magn. Reson. Imaging* **20** 540
[71] Fain S B, Korosec F R, Holmes J H, O'Halloran R, Sorkness R L and Grist T M 2007 *J. Magn. Reson. Imaging* **25** 910
[72] Liu Z, Kiessling F, Lammers T, Fokong S, Ehling J, Bornemann J and Gätjens J 2011 *Biomaterials* **32** 6155
[73] Wang C H, Kang S T and Yeh C K 2013 *Biomaterials* **34** 1852
[74] Suzukia R, Takizawaa T, Negishib Y, Hagisawac K, Tanakaa K, Sawamuraa K, Utoguchia N, Nishiokad T and Maruyama K 2007 *J. Control Release* **117** 130
[75] Liu Z, Kiessling F and Gätjens J 2010 *J. Nanomater.* **51** 1
[76] Yang F, Zhang M, He W, Chen P, Cai X, Yang L, Gu N and Wu J 2011 *Small* **7** 902
[77] Owen J, Zhou B, Rademeyer P, Tang M X, Pankhurst Q, Eckersley R and Stride E 2012 *Theranostics* **2** 1127
[78] Mulvana H, Eckersley R J, Tang M X, Pankhurst Q and Stride E 2012 *Ultrasound Med. Biol.* **38** 864